GEOCHEMISTRY

The chlorine isotope fingerprint of the lunar magma ocean

Jeremy W. Boyce,[1,2]* Allan H. Treiman,[3] Yunbin Guan,[1] Chi Ma,[1] John M. Eiler,[1] Juliane Gross,[4†] James P. Greenwood,[5] Edward M. Stolper[1]

The Moon contains chlorine that is isotopically unlike that of any other body yet studied in the Solar System, an observation that has been interpreted to support traditional models of the formation of a nominally hydrogen-free ("dry") Moon. We have analyzed abundances and isotopic compositions of Cl and H in lunar mare basalts, and find little evidence that anhydrous lava outgassing was important in generating chlorine isotope anomalies, because $^{37}Cl/^{35}Cl$ ratios are not related to Cl abundance, H abundance, or D/H ratios in a manner consistent with the lava-outgassing hypothesis. Instead, $^{37}Cl/^{35}Cl$ correlates positively with Cl abundance in apatite, as well as with whole-rock Th abundances and La/Lu ratios, suggesting that the high $^{37}Cl/^{35}Cl$ in lunar basalts is inherited from urKREEP, the last dregs of the lunar magma ocean. These new data suggest that the high chlorine isotope ratios of lunar basalts result not from the degassing of their lavas but from degassing of the lunar magma ocean early in the Moon's history. Chlorine isotope variability is therefore an indicator of planetary magma ocean degassing, an important stage in the formation of terrestrial planets.

INTRODUCTION

The Earth and Moon are nonidentical twins, born in the same giant impact (1). Chemically dissimilar from the volatile-rich rocks of Earth, rocks from the Moon are depleted in the volatile elements. This difference expresses across the entire periodic table (2), but more noticeably in the absence in lunar rocks of common terrestrial hydrous minerals such as biotite and amphibole. In contrast to those differences in elemental abundances, rocks from the Moon and Earth have very similar isotopic ratios for many of the most abundant elements (3–10), which strongly ties the two bodies together with respect to their genesis. One of the most significant exceptions to this is lunar chlorine. It recently has been shown that lunar basalts, glasses, and apatite (a common accessory mineral, $Ca_5[PO_4]_3[F,Cl,OH]$, which can contain abundant Cl) have $\delta^{37}Cl$ values [reported as $\delta^{37}Cl$ relative to standard mean ocean chlorine (SMOC)] that range from typical terrestrial values of 0 ± 1‰ to +81‰ (11, 12), far greater than observed in any other solid materials in our Solar System (11). These elevated $\delta^{37}Cl$ values were interpreted as having been produced by isotopic fractionation during extensive outgassing of Cl, probably from eruptions of basalt that were sufficiently poor in H such that HCl was not an important gas species (11). This "lava-outgassing" scenario is consistent with observations that bulk lunar rocks are generally poor in H relative to their terrestrial counterparts (13–15), but is at odds with data suggesting that many lunar magmas contained significant H before eruption (16–19), and still other data suggesting that some lunar magmas apparently had H abundances and D/H ratios similar to their terrestrial counterparts (20, 21).

It has been difficult to reconcile interpretations based on H abundances and isotopic ratios with those based on Cl abundances and

isotopic ratios, in part because there have been limited data on H and Cl abundances and isotopic compositions for the same materials. Here, we present measurements of H and Cl abundances as well as $^{37}Cl/^{35}Cl$ and D/H ratios in apatite crystals from a range of lunar basalts, where measurements are from the same thin sections and, when possible, in the same apatite crystals (for example, Fig. 1). We use these data to place constraints on the origin of the unusual chlorine isotopic composition of the Moon and to place that chlorine within the larger framework of lunar volatiles.

RESULTS

Chlorine isotope ratios in the samples analyzed here range from $\delta^{37}Cl$ = −4‰ in Miller Range (MIL) 05035 to +18‰ in 12039 (Fig. 2 and Table 1) and are consistent with the few previous analyses of $\delta^{37}Cl$ in apatite from mare basalts, with the exception of MIL 05035: The $\delta^{37}Cl$ for this sample (−4 ± 2‰) is among the lowest measured in any natural material from anywhere in the Solar System. Lunar apatites also display a wide range of D/H (Fig. 3), with δD values [reported as δD relative to Vienna standard mean ocean water (VSMOW)] of multispot grain averages ranging from −150 to +970‰. Of the basalts, 10044 has the greatest range in $\delta^{37}Cl$ (+2 to +15‰), as well as in δD, from +540 to +950‰ (n = 6), where the latter are consistent with other analyses of 10044 (Fig. 3).

Chlorine abundances in apatites from low-Ti basalts (Fig. 2A) range from 480 to 16,000 ppm. Chlorine abundances in seven of eight apatites in high-Ti basalt 10044 are between 220 and 480 ppm, with one outlier at 4000 ppm Cl. Apatite grains in low-Ti mare basalts have hydrogen concentrations (always reported here as the oxide H_2O equivalent) from below 100 ppm H_2O in sample 12040 to 2920 ppm H_2O in 12039, with data from the literature extending this to more than 5000 ppm (Fig. 2B). Apatites from high-Ti mare basalts (10044 and 75055) vary from 420 to 1430 ppm H_2O.

Lunar rocks are remarkable for their high $^{37}Cl/^{35}Cl$ values, which imply a distinctive fractionation event in lunar history that is not preserved in rocks of other planetary bodies. The lava-outgassing hypothesis of

[1]Division of Geological and Planetary Sciences, Caltech, 1200 East California Boulevard, Pasadena, CA 91125, USA. [2]Department of Earth, Planetary, and Space Sciences, University of California, Los Angeles, Los Angeles, CA 90095–1567, USA. [3]Lunar and Planetary Institute, 3600 Bay Area Boulevard, Houston, TX 77058, USA. [4]Department of Earth and Planetary Sciences, American Museum of Natural History, Central Park West at 79th Street, New York, NY 10024, USA. [5]Department of Earth and Environmental Sciences, Wesleyan University, Middletown, CT 06459, USA.
*Corresponding author. E-mail: jwboyce@alum.mit.edu
†Present address: Department of Earth and Planetary Sciences, Rutgers University, 610 Taylor Road, Piscataway, NJ 08854, USA.
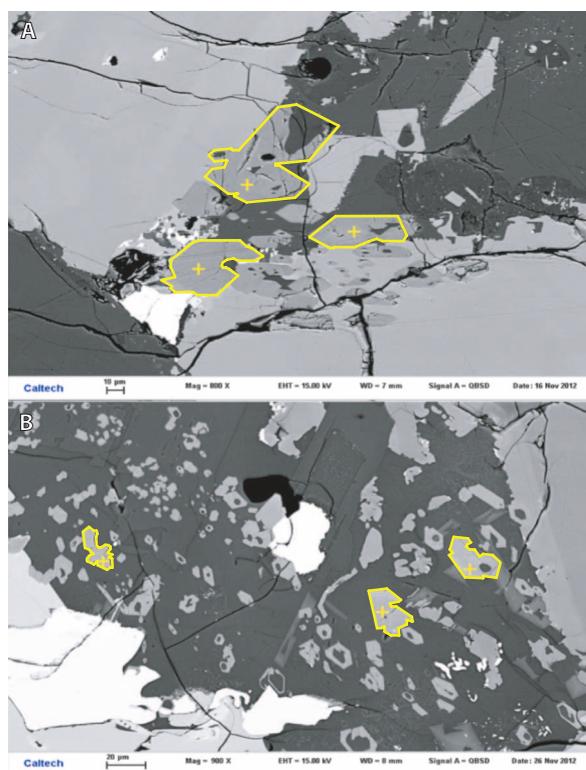
Fig. 1. Photomicrographs of two basalts. Photomicrographs of two basalts analyzed in this study, with yellow crosses marking the locations of analyses. (**A**) Subhedral apatite grains (outlined in yellow for clarity) forming a cluster in Apollo 12039,42. (**B**) Euhedral to subhedral apatite grains in Apollo 12040,211 that show skeletal growth with hollow centers.

Sharp *et al.* (*11*) requires that the basalt magmas contain minimal hydrogen (otherwise, degassing would be predicted to be of HCl gas, which would cause little fractionation of ^{37}Cl from ^{35}Cl). Independent of the mechanism of fractionating chlorine, the timing of the chlorine loss resulting in the fractionation must also be constrained: The lava-outgassing model suggests that this loss and fraction occur circa eruption.

DISCUSSION

The data reported here allow three tests of the lava-outgassing hypothesis, two based on abundances and one on isotope ratios:

(i) Elevated $^{37}Cl/^{35}Cl$ ratios should be inversely proportional to Cl abundance.

(ii) Elevated $^{37}Cl/^{35}Cl$ ratios should not be observed in samples with abundant H.

(iii) Elevated $^{37}Cl/^{35}Cl$ ratios should be observed only in samples that have enrichments in D/H.

Although the quantitative significance of measured abundances of H and Cl in apatite has been called into question (*22*), H and Cl concentrations—or even simply their presence or absence—are still valuable constraints on models used to explain observed H and Cl isotopes in lunar basalts. This is especially true of Cl, which does not experience the same order of magnitude of increase in apatite due to fractionation of fluorine.
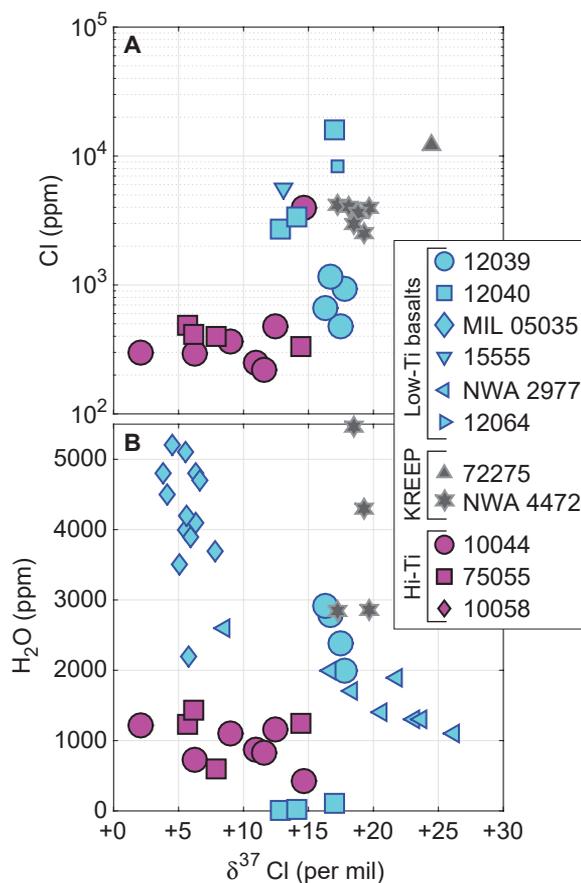

Fig. 2. Plots of Cl and H_2O versus $\delta^{37}Cl$. (**A** and **B**) Plots of Cl (A) and H_2O (B) concentrations versus $\delta^{37}Cl$ values in apatite from the Moon. Each data point represents a single apatite grain in a rock, including data from the literature plotted as smaller symbols (*11, 12, 33*); magenta symbols are high-Ti basalts; blue symbols are low-Ti basalts; gray symbols are KREEP basalts. There are no statistically significant correlations observed for any of the sample types studied here. Elevated $\delta^{37}Cl$ values are associated with both high H_2O and high Cl concentrations: The former is inconsistent with the idea that elevated $\delta^{37}Cl$ values are only associated with anhydrous conditions, and the latter is inconsistent with a simple, single-stage fractionation model.

On the basis of the lava-outgassing hypothesis, one would predict that high $\delta^{37}Cl$ values should be found preferentially in samples with low abundances of Cl, because elevated $\delta^{37}Cl$ is thought to develop only through extensive Cl loss (*11*). We find, to the contrary, that apatites with high $\delta^{37}Cl$ are among the most Cl-rich, with Cl abundances positively correlated with $\delta^{37}Cl$ values for the same samples (Fig. 2A). If the mechanism for increasing $\delta^{37}Cl$ involves preferential loss of ^{35}Cl (which seems likely, relative to ^{37}Cl) and is occurring syn- and post-eruption, there must have been a subsequent process that concentrated Cl (with elevated $\delta^{37}Cl$) relative to F and OH. This implies that the fractionation of Cl did not occur in the degassing accompanying eruption and cooling at the surface, because there is no subsequent event after eruption that can preferentially enrich high-$\delta^{37}Cl$ samples in their Cl abundance more than that same process enriches low-$\delta^{37}Cl$ samples. This is especially problematic given that the samples that are more fractionated (more elevated $\delta^{37}Cl$) likely have

Table 1. New data generated for this study.

Sample	Section	Grain	H$_2$O (ppm)	H$_2$O 2σ	Cl (ppm)	Cl 2σ	δ^{37}Cl	δ^{37}Cl 2σ	δD	δD 2σ	Category
10044	12	10	1105	29	365	104	+9	3	+933	31	High Ti basalt
10044	12	1a	728	27	292	11	+6	3	+954	27	High Ti basalt
10044	12	1b	—	—	—	—	+6	4	—	—	High Ti basalt
10044	12	1c	1220	30	300	11	+2	4	+781	23	High Ti basalt
10044	644	2	877	26	250	10	+11	3	+536	57	High Ti basalt
10044	644	8	421	22	3976	122	+15	3	—	—	High Ti basalt
10044	644	4a	826	25	219	10	+12	3	+606	33	High Ti basalt
10044	644	4b	1155	29	479	16	+12	3	+702	28	High Ti basalt
75055	55	1	604	23	398	14	+8	3	+621	35	High Ti basalt
75055	55	2	1225	35	485	16	+6	3	+794	26	High Ti basalt
75055	55	3	1241	30	334	12	+14	3	+968	27	High Ti basalt
75055	55	4	1430	34	410	14	+6	3	+794	26	High Ti basalt
75055	55	101	—	—	—	—	+5	3	—	—	High Ti basalt
12039	42	4	1996	43	928	29	+18	3	+720	30	Low Ti basalt
12039	42	6	2379	47	477	16	+17	3	+830	31	Low Ti basalt
12039	42	10	—	—	—	—	+16	3	—	—	Low Ti basalt
12039	42	11	—	—	—	—	+17	3	—	—	Low Ti basalt
12039	42	17a	2784	95	1157	36	+17	3	+729	28	Low Ti basalt
12039	42	17b	2916	57	665	21	+16	3	+698	28	Low Ti basalt
12040	211	1	105	21	15884	489	+17	3	+9	163	Low Ti basalt
12040	211	4	3	20	2689	83	+13	3	+14	84	Low Ti basalt
12040	211	5	16	20	3388	104	+14	4	−150	26	Low Ti basalt
MIL 05035	—	1	—	—	—	—	−4	2	—	—	Low Ti basalt

experienced greater degrees of fractional loss to achieve higher ^{37}Cl/^{35}Cl values—but they must finish with higher Cl abundances.

A second prediction of the lava-outgassing model is that magmas with high δ^{37}Cl should be nearly anhydrous (*11*), and thus, the apatite crystals would also be anhydrous. The negative relationship between H abundance and δ^{37}Cl in apatites from some lunar basalts (for example, NWA 2977) could be interpreted as support for this prediction (Fig. 2B). However, nearly all lunar apatites have high δ^{37}Cl relative to the range of terrestrial samples (0 ± 1‰), and many of them are rich in H, some exceeding 5000 ppm H$_2$O. Thus, although it is possible that loss of transition metal chlorides (*11*) contributes to elevated δ^{37}Cl, it does not seem possible that this signature is entirely generated by degassing from H-free melts. Whether or not this scenario is possible, there is experimental evidence suggesting that it is not necessary: evaporation of HCl at standard temperature and pressure yields an increase in +9‰ in δ^{37}Cl in the residue after 90% evaporation (*23*). Therefore, it is not impossible to achieve fractionations of the same order of magnitude as those observed in mare basalts from phase transformations of HCl.

Third, we note that if the H-poor magmas required for generation of δ^{37}Cl anomalies were themselves generated by extensive degassing of H$_2$ (favoring the lighter isotope), one should expect that mare basalts with elevated δ^{37}Cl would also have relatively elevated δD. This is not only because—in the context of the lava-outgassing hypothesis—extensive loss of hydrogen is required to generate conditions under which metal chloride degassing dominates over HCl degassing, but also (more generally) because magmas that have outgassed Cl should also have had the opportunity to outgas H. If the building blocks of Earth and its Moon were H-bearing, and the lava-outgassing hypothesis requires the magma to be H-free when Cl loss is initiated syn-eruption, then hydrogen must have been lost before Cl, resulting in an elevated D/H ratio in the residue. This expectation is not met: Instead of the positive correlation one might expect, lunar basalts actually define two separate populations with no apparent relationship between δD and δ^{37}Cl: Some basalts with very high δ^{37}Cl (for example, samples 12040 and NWA 2977, which range up to +20‰) have low δD (≤0‰) (Fig. 4).

It should also be noted that neither the relationship between δD and H abundance (Fig. 3) nor the presence of apatite with strongly
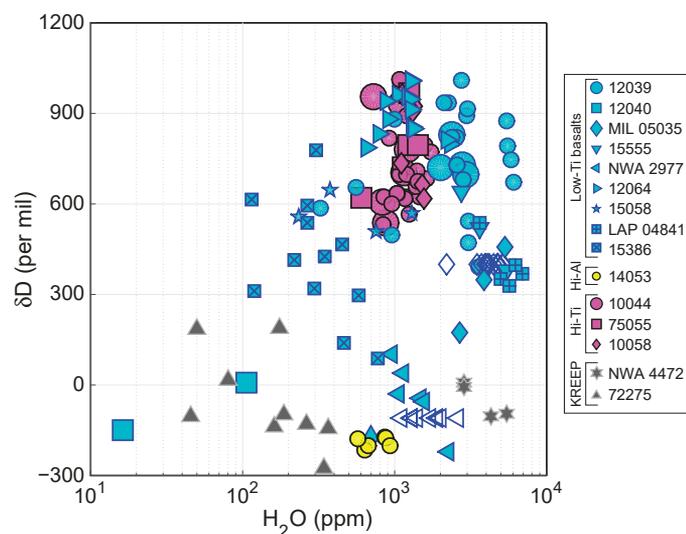
Fig. 3. δD versus H₂O. δD versus H₂O for new data (large symbols) and data from the literature (small symbols). Hollow symbols are multiple hydrogen abundance measurements plotted with bulk δD values. Data have been previously interpreted as representing mixing between a high-δD, high-H₂O end member (possibly comets), and a low-δD, low-H₂O end member (possibly solar wind), or evolution from or contamination with a material of chondritic composition (16, 24, 25, 33), though neither explanation explains all the data. Note the large number of analyses with δD values in the range for bulk chondrites (+750 to −200‰) (58).

Fig. 4. Plot of δD versus δ³⁷Cl. Plot of δD versus δ³⁷Cl for data generated in this study and those from previous studies (plotted as smaller symbols). Hollow symbols indicate in situ δ³⁷Cl measurements plotted versus bulk or mean apatite δD from the literature. The presence of high δ³⁷Cl apatite with low δD values is inconsistent with the prediction that elevated δ³⁷Cl would accompany elevated δD, because both isotopes should shift toward higher δ values during degassing. The lack of correlation between δD and δ³⁷Cl suggests that the two isotope systems are at least partially decoupled and that multiple processes may be at work.

negative δD can be explained by extensive losses of H_2 from a chondritic reservoir (24, 25). Given the presence of implanted solar wind, spallogenic D, and H-rich chondritic materials gardened into the upper lunar regolith through repeated impacts, it is plausible that the regolith serves as an exchangeable reservoir of H for adjacent magmatic dikes, sills, and lava flows that can modify the D/H ratio of magmas (26, 27). This form of "crustal contamination" [as previously suggested by Hui et al. (28) to explain major and trace element variability in Apollo 14 basalts] may exert significant leverage on D/H ratios, especially in magmas with low intrinsic H abundances. Apatite grains in individual basalt samples show wide ranges of δD values, with individual samples having ranges as large as 800‰ (10044), which is also consistent with partial late-stage reequilibration with extrinsic hydrogen.

We conclude that none of the three tests of the lava-outgassing hypothesis are consistent with this new data set, and therefore, we develop other explanations, focusing on processes that are implied by correlations between d37Cl and other geochemical properties: The δ³⁷Cl values of apatite from lunar basalts are correlated with Cl content, which is known to be enriched in KREEP. KREEP is the name given to a chemical component—possibly derived from the urKREEP, the last vestige of the lunar magma ocean—rich in potassium (K), the rare earths (REE), and phosphorus (P) and other elements that are incompatible during the crystallization of magmas (29–31). Incompatible elements are those that are preferentially excluded from crystals growing from a melt and therefore concentrated in that residual melt—in this case, the lunar magma ocean. The lunar magma ocean first crystallizes from below, then from both above and below, resulting in a "sandwich horizon" of melt with decreasing volume and increasing abundances of incompatible elements (31). KREEP (and the proposed urKREEP source) have long been implicated in the trace element variations of lunar basalts
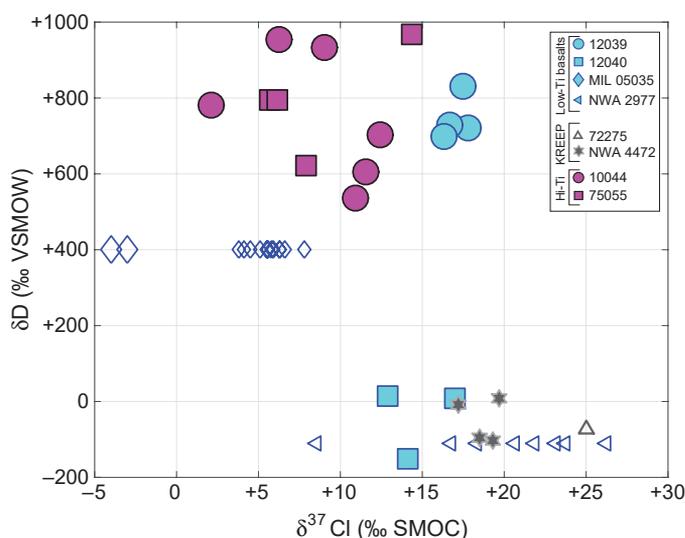
[for example, (32)], with different units having different contributions of KREEP (sometimes referred to as "KREEPiness"). More KREEP-rich (or "KREEPy") samples are observed to have higher abundances of trace elements such as Th, Cl, as well as the major and trace elements that make up the acronym KREEP. Model compositions of the urKREEP (29) also indicate that the urKREEP may have elevated La/Lu ratios, relative to the mare basalt source. Thus, trace element abundances and ratios can be used to determine the magnitude of KREEP contamination/addition. The δ³⁷Cl values of mare basalt apatites are also positively correlated with abundances and ratios in their host rocks of the elements that are enriched in the lunar KREEP component, notably bulk Th abundance and La/Lu abundance ratios derived from the literature (Fig. 5) (29, 31).

The correlations between Cl, Th, La/Lu, and δ³⁷Cl suggest that Cl abundances and δ³⁷Cl of mare basalts are controlled—at least in part—by the abundance of the KREEP component. The highest values of δ³⁷Cl found in previous studies for apatite from lunar basalt were from a KREEPy clast in the highlands breccia 72275 (11), whereas the highest values observed by (33) were also in a KREEPy clast. The trends in Fig. 5 are consistent with the existence of a background lunar mantle reservoir containing Cl with a δ³⁷Cl value similar to the bulk Earth (~0‰) and a KREEP reservoir such as urKREEP containing more abundant Cl with a δ³⁷Cl of ≥+30‰ (34). The lunar mantle end member might be recording an undegassed lunar source, a partially degassed source that did not have the special conditions required for fractionation of Cl isotopes, or meteoritic material that could have a δ³⁷Cl as low as −4‰ (35). Chlorine degassed from a mare basalt at any stage of lunar evolution might be expected to have low δ³⁷Cl relative to its source and could return to the Moon as adsorbates on regolith grains (11), providing another possible explanation for the negative δ³⁷Cl values observed for lunar apatite in MIL 05035.
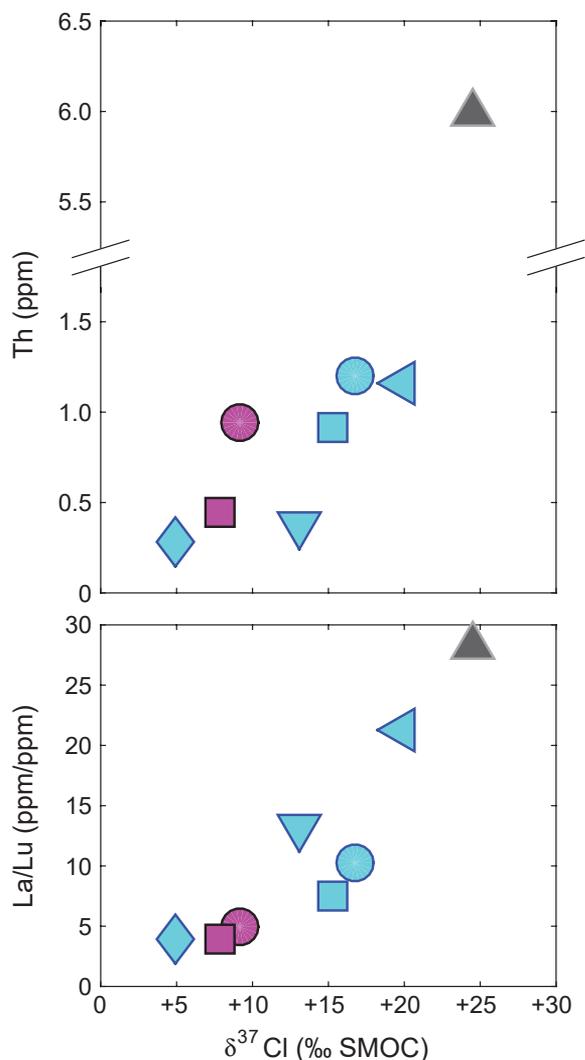
Fig. 5. Bulk Th and La/Lu versus δ^{37}Cl. (A and B) Measures of KREEP contribution, bulk rock Th abundance (A), and bulk rock La/Lu (B), as a function of δ^{37}Cl, with trace element data from (43, 54, 59). Symbols are the same as those in previous figures. For all basalts, δ^{37}Cl is strongly correlated with Th and La/Lu, suggesting that pure urKREEP would have δ^{37}Cl $\geq$+30‰.

We interpret the high δ^{37}Cl of urKREEP to have formed during vapor phase loss of Cl from the magma ocean, perhaps by a mechanism akin to that of Sharp *et al.* (11): loss of transition metal chlorides from a hydrogen-poor melt. However, it is also possible that the mechanism is that of HCl loss, which was also put forth by Sharp *et al.* (23). Either mechanism of Cl loss is consistent with recent interpretations of Cl, Zn, and K isotopes from lunar materials, subsets of which have similar patterns of fractionations (36). Chlorine that survives the degassing of the lunar magma ocean is enriched in ^{37}Cl relative to ^{35}Cl, and is then concentrated into the urKREEP, because Cl is incompatible in all of the major lunar mantle phases and will choose to stay in the ever-shrinking remnants of the lunar magma ocean. This results in a reservoir that is enriched in Cl and Th, has elevated La/Lu, and still has the fingerprint of the magma ocean degassing preserved in the elevated isotopic ratio of Cl. Basalts may acquire this isotopic signature via incorporation of KREEP-

rich materials in the lunar mantle or as the magmas are traversing—and assimilating—crust or regolith materials that have a KREEP signature.

Other planets are inferred to have had magma oceans early in their histories—including Earth—which shows no evidence of elevated δ^{37}Cl (37). It is of course possible that the budget of Cl on Earth is dominated by late delivery of volatile-rich materials (38), but this is inconsistent with the argument that the terrestrial planets received their hydrogen early (39). Even if Earth's chlorine is primordial, the pressure, temperature, and chemistry of the atmosphere above a magma ocean most likely control—at least in part—the extent to which loss can change the isotope ratio of the residuum (40, 41). To the extent that fractionation due to Cl loss is governed by parent body size—with smaller bodies predicted to have less atmosphere and therefore larger potential fractionations—the magnitudes (if not the directions) of the δ^{37}Cl anomalies for rocks from Earth, Mars, and the Moon are consistent with the relative size and expected atmospheric pressures of those bodies during their magma ocean phases. This model predicts elevated δ^{37}Cl for other small bodies that had magma oceans, as is inferred for 4Vesta (42). Thus, chlorine isotopes may provide a unique tool for exploring the existence, extent, and conditions during the magma ocean phase that is thought to be a significant stage in the formation of terrestrial planetary bodies.

MATERIALS AND METHODS

Experimental design

The purpose of this study was to investigate the relationship between chlorine and other elements (as well as their isotope ratios) in lunar basalts. We set out to test the hypothesis that δ^{37}Cl variations in lunar basalts are due to anhydrous degassing of basalts during eruption (11). Three predictions following from that hypothesis were tested:

(i) Elevated ^{37}Cl/^{35}Cl ratios should be inversely proportional to Cl abundance.

(ii) Elevated ^{37}Cl/^{35}Cl ratios should not be observed in samples with abundant H.

(iii) Elevated ^{37}Cl/^{35}Cl ratios should be reserved for samples that have enrichments in D/H.

These hypotheses were tested by making the H, Cl, D/H, and ^{37}Cl/^{35}Cl measurements in apatite crystals from the same samples and, when possible, in the same crystals. After these predictions were tested, additional hypotheses were formulated, including the hypothesis that the degassing of the lunar magma ocean had generated the high ^{37}Cl/^{35}Cl ratios observed in the samples. This hypothesis makes three additional predictions:

(i) Elevated ^{37}Cl/^{35}Cl ratios should be positively correlated to Cl abundance.

(ii) Elevated ^{37}Cl/^{35}Cl ratios should be positively correlated to Th abundance, which is elevated in urKREEP.

(iii) Elevated ^{37}Cl/^{35}Cl ratios should be positively correlated to La/Lu ratio, which is elevated in urKREEP.

These predictions were tested by direct measurement of δ^{37}Cl and Cl abundance (above), and by comparison with literature values for bulk Th content and La/Lu ratio.

Materials

Six thin sections of five samples were analyzed by ion microprobe for this study: two high-Ti basalts (10044 and 75055) and three low-Ti basalts (12039, 12040, and MIL 05035).

Apollo sample 10044. This is a low-K ilmenite basalt that has a Ti content lower than typical ilmenite basalts from Apollo 11 (43). On the basis of its texture, it was classified as coarse-grained porphyritic basalt (44) and microgabbro [for example, (45)], which consists of subhedral to anhedral pyroxene, set in a matrix of plagioclase, anhedral pyroxene, and ilmenite, with minor apatite, spinel, silica, and symplectitic intergrowth. For a more detailed description of the petrography of 10044, see the Lunar Sample Compendium (43). Here, apatites from two thin sections were examined, 10044,12 and 10044,644, which appear mostly as inclusions in pyroxene and oxides. The grain sizes range from <5 to 200 μm. Most grains are euhedral to subhedral in shape, with some grains appearing as irregular-shaped aggregates. For this study, five apatite grains were analyzed (31 analyses total) with ranges in grain size from 20 to 200 μm.

Apollo sample 75055. This is a medium-grained ilmenite basalt that is more aluminous and less Ti-rich than other Apollo 17 basalts (46). On the basis of its texture, the sample has been described as subophitic (44, 47) with tabular plagioclase intergrown with subhedral to anhedral pyroxene and ilmenite laths. For further petrographic information, see the Lunar Sample Compendium (43). Here, Apollo sample 75055,55 was analyzed. Apatite in this sample appears as inclusions mainly in pyroxene and oxides, but some can be found in plagioclase. Apatite ranges in grain size from <5 to 110 μm and are mostly subhedral in shape. Some grains show skeletal growth with hollow centers similar to apatite from Apollo 12040 (Fig. 1). Five apatite grains have been analyzed for this study (13 analyses total), none smaller than 10 μm in size.

Apollo sample 12039. This is a medium-grained pigeonite basalt/microgabbro (48, 49) and one of the most Fe-rich and Mg-poor Apollo 12 igneous rocks (50). Texturally, it ranges from porphyritic (44), to subophitic, to granular (50). Petrographically, it is mainly composed of plagioclase and pyroxene with long needles of ilmenite and tridymite cutting across the plagioclase and pyroxene. Minor troilite, tranquillityite, chromite, metal, apatite, and symplectitic intergrowths are present (43). Here, apatite in thin section 12039,42 was analyzed. Apatite is subhedral to anhedral, sometimes present as long needles, with grain sizes ranging from <10 to 400 μm long. Some grains occur as clusters, and some grains show skeletal growth (Fig. 1). Seventeen points in five different grains were analyzed.

Apollo sample 12040. This is a coarse-grained olivine basalt with a high proportion of mafic minerals. Texturally, it is equigranular with an average grain size of 1 mm (51). It is mainly composed of olivine and pyroxene with minor plagioclase, ilmenite, chromite, troilite, metal, phosphates, and alkali feldspar (52, 53). Here, three apatite grains were analyzed (14 spots total) in thin section 12040,211. Apatite is mostly subhedral to anhedral, and grain sizes range from <5 to 30 μm and occurs in pyroxene and plagioclase. Small, subhedral to euhedral apatite grains show skeletal growth with hollow centers (Fig. 1).

Lunar meteorite MIL 05035. MIL 05035 is a coarse-grained lunar gabbroic meteorite (54). It mainly consists of pyroxene (54 to 69 volume %) with grain sizes up to 6 mm and plagioclase (17 to 36 volume %) with grain sizes up to 4 mm. It contains minor fayalitic olivine, ilmenite, spinel, FeS, apatite, and silica, which represent crystallized products of its residual melt (54, 55). It also contains symplectic intergrowth that is composed of silica, fayalitic olivine, and hedenbergitic pyroxene (54). Here, a single apatite grain in the thin section MIL 05035,6 was analyzed (two points total).

Methods

Measurements of H, Cl, F, as well as D/H and $^{37}Cl/^{35}Cl$ were all made in the Caltech Center for Microanalysis using the Cameca 7f-GEO secondary ion mass spectrometer. Standards used for abundance measurements are those described in (56) with the slightly revised values of (57). Isotopic measurements are reported relative to Durango apatite at $\delta^{37}Cl = +0.40$‰ SMOC and $\delta D = -120 \pm 5$‰ VSMOW (2σ) (16).

Abundances of OH, F, and Cl. Measurements of volatile abundances in lunar apatite are made by measuring $^{16}O^1H$, ^{18}O (reference element), ^{19}F, ^{31}P (secondary reference element), ^{32}S, and ^{35}Cl using a −0.5-nA, 10-keV Cs^+ beam at a mass resolving power of ~5500, sufficient to separate peaks of interest from all known interferences (18). Preanalytical sputtering was performed with a 2-nA beam and 25-μm × 25-μm raster for 300 s, except in cases where abundance measurements followed isotopic measurements, in which case preanalytical sputtering was reduced to 20 s. This was followed by 10 to 30 cycles of measurement with a 2-μm × 2-μm raster. Secondary ions were accelerated to −9 keV, and those passing through a ~100-μm field aperture were measured with dynamic transfer via electron multiplier, except for F and Cl, that in some cases were measured with a Faraday cup. An 80% electronic gating was applied to further reduce contamination. Measurements of less than 100 ppm H_2O are very conservatively assumed to be within error of the blank for epoxy-bearing thin sections such as those studied here.

Cl isotopes. Measurements of Cl isotopes were made in two sessions, both normalized to Durango apatite at +0.4‰ SMOC. In the first session, samples were presputtered for 300 s at ~2 nA with a 25-μm × 25-μm raster. Data were collected for ^{35}Cl (1 s) and ^{37}Cl (1 s) using a lower primary beam current (~0.5 nA), rastered over a smaller area (2 μm × 2 μm) for 300 cycles. Data were collected with an electron multiplier (dead time = 44 ns) at low mass resolving power (~2000). Additional settings were as follows: field aperture (400 μm), contrast aperture (150 μm), no dynamic transfer, no E-gating, 45-eV energy window. The second session used similar settings, except that a Faraday cup detector was used instead of an electron multiplier, with a higher primary current (~3 to 3.5 nA for the presputter, ~1.5 to 2 nA), and shorter analysis times (120-s presputter, 30 cycles of measurement). No difference was observed in the reproducibility of the reference materials between the two sessions.

H isotopes. Measurements of H isotopes were made at low mass resolution [mass resolution power (MRP) ~800] with the electron multiplier, with 50 to 100 cycles of ~3-nA, 2-μm × 2-μm rastered beam sputtering, preceded by 180 s of ~3-nA, 25-μm × 25-μm raster presputtering. Durango apatite was used as a δD standard, with a value of −120‰ VSMOW (16). Additional settings include the following: field aperture of 100 μm, no dynamic transfer, electronic gating of 80% (64% by area).

Statistical analysis

All uncertainties are reported as 2 SEMs. For single analyses, uncertainties are reported as 2 SEMs, which consists of the analytical uncertainty. For multiple analyses of the same sample, it consists of either the analytical uncertainty (2 SEMs) or two standard deviations of the mean of the measured values for that sample, whichever is larger. For measurements of hydrogen abundance (always reported as H_2O, regardless of speciation), all values below 100 ppm H_2O are assumed to be within error of zero, because all of our samples are epoxy-bearing thin sections, which are not ideal for low-blank H_2O measurements by ion microprobe. No outliers were discarded: The only data not reported here are due to operator error on the instrument and are noted before data reduction.

Boyce *et al. Sci. Adv.* 2015;1:e1500380   25 September 2015

6 of 8

REFERENCES AND NOTES

1. W. K. Hartmann, D. R. Davis, Satellite-sized planetesimals and lunar origin. *Icarus* **24**, 504–515 (1975).

2. F. Albarede, E. Albalat, C.-T. A. Lee, An intrinsic volatility scale relevant to the Earth and Moon and the status of water in the Moon. *Meteorit. Planet. Sci.* **50**, 568–577 (2015).

3. U. Wiechert, A. N. Halliday, D. C. Lee, G. A. Snyder, L. A. Taylor, D. Rumble, Oxygen isotopes and the Moon-forming giant impact. *Science* **294**, 345–348 (2001).

4. M. D. Norman, G. M. Yaxley, V. C. Bennett, A. D. Brandon, Magnesium isotopic composition of olivine from the Earth, Mars, Moon, and pallasite parent body. *Geophys. Res. Lett.* **33**, L15202 (2006).

5. M. Touboul, T. Kleine, B. Bourdon, H. Palme, R. Wieler, Late formation and prolonged differentiation of the Moon inferred from W isotopes in lunar metals. *Nature* **450**, 1206–1209 (2007).

6. M. J. Spicuzza, J. M. D. Day, L. A. Taylor, J. W. Valley, Oxygen isotope constraints on the origin and differentiation of the Moon. *Earth Planet. Sci. Lett.* **253**, 254–265 (2007).

7. J. Simon, D. J. DePaolo, Stable calcium isotopic composition of meteorites and rocky planets. *Earth Planet. Sci. Lett.* **289**, 457–466 (2010).

8. C. Fitoussi, B. Bourdon, Silicon isotope evidence against an enstatite chondrite Earth. *Science* **335**, 1477–1480 (2012).

9. J. Zhang, N. Dauphas, A. M. Davis, I. Leya, A. Fedkin, The proto-Earth as a significant source of lunar material. *Nat. Geosci.* **5**, 251–255 (2012).

10. D. Herwartz, A. Pack, B. Friedrichs, A. Bischofff, Identification of the giant impactor Theia in lunar rocks. *Science* **344**, 1146–1150 (2014).

11. Z. D. Sharp, C. K. Shearer, K. D. McKeegan, J. D. Barnes, Y. Q. Wang, The chlorine isotope composition of the Moon and implications for an anhydrous mantle. *Science* **329**, 1050–1053 (2010).

12. Y. Wang, Y. Guan, W. Hsu, J. M. Eiler, paper presented at the 75th Annual Meteoritical Society Meeting, Cairns, Queensland, Australia, 2012.

13. S. Epstein, H. P. Taylor, The isotopic composition and concentration of water, hydrogen, and carbon in some Apollo 15 and 16 soils and in the Apollo 17 orange soil, *Proceedings of the 4th Lunar Science Conference*, Houston, TX, 5 to 8 March 1973 (Pergamon Press Inc., New York, 1973).

14. L. Haskin, P. H. Warren, in *Lunar Sourcebook* (Cambridge Univ. Press, Cambridge, 1991), pp. 357–474.

15. J. Papike, L. Taylor, S. Simon, Lunar minerals, *Lunar Sourcebook* (Cambridge Univ. Press, Cambridge, 1991), pp. 121–181.

16. J. P. Greenwood, S. Itoh, N. Sakamoto, P. Warren, L. Taylor, H. Yurimoto, Hydrogen isotope ratios in lunar rocks indicate delivery of cometary water to the Moon. *Nat. Geosci.* **4**, 79–82 (2011).

17. F. M. McCubbin, A. Steele, E. H. Hauri, H. Nekvasilc, S. Yamashita, R. J. Hemley, Nominally hydrous magmatism on the Moon. *Proc. Natl. Acad. Sci. U.S.A.* **107**, 11223–11228 (2010).

18. J. W. Boyce, Y. Liu, G. R. Rossman, Y. Guan, J. M. Eiler, E. M. Stolper, L. A. Taylor, Lunar apatite with terrestrial volatile abundances. *Nature* **466**, 466–469 (2010).

19. H. Hui, A. H. Pelsier, H. Zhang, C. R. Neal, Water in lunar anorthosites and evidence for a wet early Moon. *Nat. Geosci.* **6**, 177–180 (2013).

20. A. E. Saal, E. H. Hauri, M. L. Cascio, J. A. Van Orman, M. C. Rutherford, R. F. Cooper, Volatile content of lunar volcanic glasses and the presence of water in the Moon's interior. *Nature* **454**, 192–195 (2008).

21. A. E. Saal, E. H. Hauri, J. A. Van Orman, M. C. Rutherford, Hydrogen isotopes in lunar volcanic glasses and melt inclusions reveal a carbonaceous chondrite heritage. *Science* **340**, 1317–1320 (2013).

22. J. W. Boyce, S. M. Tomlinson, F. M. McCubbin, J. P. Greenwood, A. H. Treiman, The lunar apatite paradox. *Science* **344**, 400–402 (2014).

23. Z. D. Sharp, J. D. Barnes, T. P. Fischer, M. Halick, An experimental determination of chlorine isotope fractionation in acid systems and applications to volcanic fumaroles. *Geochim. Cosmochim. Acta* **74**, 264–273 (2010).

24. J. J. Barnes, I. A. Franchi, M. Anand, R. Tartèse, N. A. Starkey, M. Koike, Y. Sano, S. S. Russell, Accurate and precise measurements of the D/H ratio and hydroxyl content in lunar apatites using NanoSIMS. *Chem. Geol.* **337–338**, 48–55 (2013).

25. R. Tartese, M. Anand, Late delivery of chondritic hydrogen into the lunar mantle: Insights from mare basalts. *Earth Planet. Sci. Lett.* **361**, 480–486 (2013).

26. M. Rumpf, S. A. Fagents, I. A. Crawford, K. A. Joy, Numerical modeling of lava-regolith heat transfer on the Moon and implications for the preservation of implanted volatiles. *J. Geophys. Res. Planets* **118**, 382–397 (2013).

27. A. Stephant, F. Robert, The negligible chondritic contribution in the lunar soils water. *Proc. Natl. Acad. Sci. U.S.A.* **111**, 15007–15012 (2014).

28. H. Hui, J. G. Oshrin, C. R. Neal, Investigation into the petrogenesis of Apollo 14 high-Al basaltic melts through crystal stratigraphy of plagioclase. *Geochim. Cosmochim. Acta* **75**, 6439–6460 (2011).

29. C. R. Neal, L. A. Taylor, Metasomatic products of the lunar magma ocean: The role of KREEP dissemination. *Geochim. Cosmochim. Acta* **53**, 529–541 (1989).

30. B. Jolliff, paper presented at the 20th Lunar and Planetary Science Conference, Houston, TX, 1989.

31. P. H. Warren, J. T. Wasson, The origin of KREEP. *Rev. Geophys.* **17**, 73–88 (1979).

32. G. W. J. Reed, S. Jovanovic, L. Fuchs, Trace element relations between Apollo 14 and 15 and other lunar samples, and the implications of a moon-wide Cl-KREEP coherence and Pt-metal noncoherence. *Proc. Third Lunar Sci. Conf.* **2**, 1989–2001 (1972).

33. R. Tartèse, M. Anand, K. H. Joy, I. A. Franchi, H and Cl isotope systematics of apatite in brecciated lunar meteorites Northwest Africa 4472, Northwest Africa 773, Sayh al Uhaymir 169, and Kalahari 009. *Meteorit. Planet. Sci.* **49**, 2266–2289 (2014).

34. A. H. Treiman, J. W. Boyce, J. Gross, Y. Guan, J. M. Eiler, E. M. Stolper, Phosphate-halogen metasomatism of lunar granulite 79215: Impact-induced fractionation of volatiles and incompatible elements. *Am. Mineral.* **99**, 1860–1870 (2014).

35. J. T. Williams, Z. D. Sharp, C. K. Shearer, C. B. Agee, paper presented at the 46th Lunar and Planetary Science Conference, Houston, TX, 2015.

36. J. M. D. Day, F. Moynier, Evaporative fractionation of volatile stable isotopes and their bearing on the origin of the Moon. *Philos. Trans. R. Soc. A* **372**, 20130259 (2014).

37. Z. D. Sharp, C. K. Shearer, F. M. McCubbin, C. Agee, K. D. McKeegan, paper presented at the 44th Lunar and Planetary Science Conference, Houston, TX, 2013.

38. Z. Wang, H. Becker, Ratios of S, Se and Te in the silicate Earth require a volatile-rich late veneer. *Nature* **499**, 328–331 (2013).

39. A. Sarafian, H. Marschall, S. Nielsen, F. McCubbin, B. Monteleone, 45th Lunar and Planetary Institute Science Conference, Houston, TX, 2014.

40. F. M. Richter, A. M. Davis, D. S. Ebel, A. Hashimoto, Elemental and isotopic fractionation of type B calcium-, aluminum-rich inclusions: Experiments, theoretical considerations, and constraints on their thermal evolution. *Geochim. Cosmochim. Acta* **66**, 521–540 (2002).

41. E. D. Young, A. Galy, The isotope geochemistry and cosmochemistry of magnesium. *Rev. Mineral. Geochem.* **55**, 197–230 (2004).

42. K. Righter, M. J. Drake, A magma ocean on Vesta: Core formation and petrogenesis of eucrites and diogenites. *Meteorit. Planet. Sci.* **32**, 929–944 (1997).

43. C. Meyer, *Lunar Sample Compendium* (NASA, Houston, TX, 2009).

44. P. E. McGee, J. L. Warner, C. H. Simonds, Introduction to the Apollo Collections. Part 1: Lunar Igneous Rocks (NASA, Washington, DC, 1977).

45. J. V. Smith et al., paper presented at the Apollo 11 Lunar Science Conference, Houston, TX, 1970.

46. J. M. Rhodes et al., paper presented at the 7th Lunar Science Conference, Houston, TX, 1976.

47. R. F. Dymek, A. L. Albee, A. A. Chodos, paper presented at the 6th Lunar and Planetary Science Conference, Houston, TX, 1975.

48. J. M. Rhodes, D. P. Blanchard, M. A. Dungan, J. C. Brannon, K. V. Rodgers, paper presented at the 8th Lunar and Planetary Science Conference, Houston, TX, 1977.

49. C. R. Neal, M. D. Hacker, G. A. Snyder, L. A. Taylor, Y.-G. Liu, R. A. Schmitt, Basalt generation at the Apollo 12 site, Part 2: Source heterogeneity, multiple melts, and crustal contamination. *Meteoritics* **29**, 349–361 (1994).

50. T. E. Bunch, K. Keil, M. Prinz, Mineralogy, petrology and chemistry of lunar rock 12039. *Meteoritics* **7**, 245–255 (1972).

51. P. E. Champness, A. C. Dunham, F. G. F. Gibb, H. N. Giles, W. S. MacKenzie, E. F. Stumpel, J. Zussman, paper presented at the 2nd Lunar and Planetary Science Conference, Houston, TX, 1971.

52. B. M. French, L. S. Walter, K. F. J. Heinrich, P. D. Lowman Jr., A. S. Doan Jr., I. Adler, *Compositions of Major and Minor Minerals in Five Apollo 12 Crystalline Rocks* (NASA, Greenbelt, MD, 1972).

53. G. M. Brown, C. H. Emeleus, J. G. Holland, A. Peckett, R. Phillips, paper presented at the 2nd Lunar Science Conference, Houston, TX, 1971.

54. K. H. Joy, I. A. Crawford, M. Anand, R. C. Greenwood, I. A. Franchi, S. S. Russell, The petrology and geochemistry of Miller Range 05035: A new lunar gabbroic meteorite. *Geochim. Cosmochim. Acta* **72**, 3822–3844 (2008).

55. T. Arai, B. R. Hawke, T. A. Giguere, K. Misawa, M. Miyamoto, H. Kojima, Antarctic lunar meteorites Yamato-793169, Asuka-881757, MIL 05035, and MET 01210 (YAMM): Launch pairing and possible cryptomare origin. *Geochim. Cosmochim. Acta* **74**, 2231–2248 (2010).

56. F. M. McCubbin, E. H. Hauri, S. M. Elardo, K. E. Vander Kaaden, J. Wang, C. K. Shearer Jr., Hydrous melting of the martian mantle produced both depleted and enriched shergottites. *Geology* **40**, 683–686 (2012).

57. J. W. Boyce, J. M. Eiler, M. C. Channon, An inversion-based self-calibration for SIMS measurements: Application to H, F, and Cl in apatite. *Am. Mineral.* **97**, 1116–1128 (2012).

58. C. M. O. D. Alexander, R. Bowden, M. L. Fogel, K. T. Howard, C. D. K. Herd, L. R. Nittler, The provenances of asteroids, and their contributions to the volatile inventories of the terrestrial planets. *Science* **337**, 721–723 (2012).

59. K. Righter, J. Gruener, Northwest Africa 773, 2700, 2727, 2977, 3160, *The Lunar Meteorite Compendium*; http://curator.jsc.nasa.gov/antmet/lmc/index.cfm.

Citation: J. W. Boyce, A. H. Treiman, Y. Guan, C. Ma, J. M. Eiler, J. Gross, J. P. Greenwood, E. M. Stolper, The chlorine isotope fingerprint of the lunar magma ocean. *Sci. Adv.* **1**, e1500380 (2015).

Boyce *et al. Sci. Adv.* 2015;1:e1500380   25 September 2015

8 of 8

Science Advances

The chlorine isotope fingerprint of the lunar magma ocean

Jeremy W. Boyce, Allan H. Treiman, Yunbin Guan, Chi Ma, John M. Eiler, Juliane Gross, James P. Greenwood and Edward M. Stolper

ARTICLE TOOLS	http://advances.sciencemag.org/content/1/8/e1500380
REFERENCES	This article cites 41 articles, 13 of which you can access for free http://advances.sciencemag.org/content/1/8/e1500380#BIBL
PERMISSIONS	http://www.sciencemag.org/help/reprints-and-permissions

Use of this article is subject to the Terms of Service